# Inhomogeneous Broadening and Rotational Relaxation Effects in a Molecular Gas Flow Laser

J.S. Goela,* J.J. Healy,† and T.F. Morse‡
*Brown University, Providence, R.I.*

**Kinetic equations have been formulated and solved to assess the significance of inhomogeneous broadening and rotational relaxation on a class of molecular flow lasers. In particular, criteria for the region of validity of a rate equation formalism are obtained, and the effect of departures from a Boltzmann distribution of rotational states is discussed. This investigation extends previous work by Cool on the gas flow molecular laser to include collisional diffusion in velocity space as well as finite rotational relaxation. Both high and low pressure effects on laser performance characteristics are studied in detail.**

## Nomenclature

$A_{ijk\ell}$ = Einstein coefficient for transition $i_j \leftrightarrow k_\ell$
$a$ = the cavity loss parameter
$a_1$ = the fraction of molecules of group 1 that are in the terminal lasing level, = 0.04
$B$ = Boltzmann factor for level 2, $(n_{2J}/n_2)_{eqm}$
$B_1$ = Boltzmann factor for level 1, $(n_{1J+1}/n_1)_{eqm}$
$B''$ = rotational constant for upper lasing level
$B'$ = rotational constant for lower lasing level
$b$ = dimensionless ratio of collisional line width to Doppler width, $\equiv \Delta\nu_H(\ell n 2)^{1/2}/2\Delta\nu_D$
$c$ = velocity of light, m/sec
$E$ = the energy density per unit cavity volume, $mJ/cm^3$
$\mathrm{erf}(b)$ = error function of argument $b$,

$$\equiv 2/\sqrt{\pi}\int_0^b \exp(-x^2)\,dx$$

$f_i$ = velocity distribution function of $i$th vibrational level
$f_{ij}$ = velocity distribution function for $j$th rotational state of $i$th vibrational level
$f_\nu$ = photon distribution function
$G(0)$ = gain coefficient at line center, $cm^{-1}$
$G(\zeta_{2J1J+1})$ = gain coefficient for nondimensional frequency $\zeta_{2J1J+1}$, $cm^{-1}$
$H$ = height of the cavity
$H_{21}(f_{1J+1})$ = the number of particles per unit volume, per unit solid angle about $\ell$ capable of absorbing a photon on a line centered about $\nu_{2J1J+1}$, $\equiv \int_{-\infty}^{\infty} f_{1J+1} q_{2J1J+1}\,d\xi$
$H(z)$ = the Heavyside unit step function of argument $z$
$h$ = Planck's constant, joules-sec
$I$ = the local (two way) radiation intensity, watts/cm²
$I^*$ = integrated radiation intensity,

$$\equiv 1/L\int_0^L I\,dx,\ \text{watts/cm}^2$$

$I_S^*$ = local saturation parameter, watts/cm²
$J$ = rotational quantum number of upper laser level, = 18 for $CO_2$ at 300K
$J+1$ = rotational quantum number of lower laser level, = 19 for $CO_2$ at 300K
$K_{ij}$ = rate constants for relaxation between vibrational levels $i$ and $j$, $sec^{-1}\,torr^{-1}$
$K_{ijk}$ = rate constant for relaxation between $j$th rotational state of $i$th vibrational level and vibrational level $k$, $sec^{-1}\,torr^{-1}$
$k$ = Boltzmann's constant, joule/molecule K
$L$ = length of laser cavity perpendicular to flow direction, meters
$L(z)$ = nondimensional laser intensity as a function of position $z$
$\ell$ = a unit vector
$\ell_x, \ell_y, \ell_z$ = three components of unit vector $\ell$
$M_{ij}$ = Maxwellian velocity distribution function, $\equiv k_{ij}/K_{ji}(1/2\pi RT_0)^{3/2}\exp(-\eta^2)n_i$
$n_i$ = number density for vibrational level $i$, molecules/cm³
$n_{ij}$ = number density for $j$th rotational state of $i$th vibrational level, molecules/cm³
$n_{2x}$ = number of molecules in vibrational level 2 minus those whose rotational state is involved in stimulated emission at the lasing frequency $\equiv n_2 - n_{2J}$, molecules/cm³
$P$ = total power output, watts
$P_{max}$ = maximum power output, watts
$q_{2J1J+1}$ = line shape function for transition $2_J \leftrightarrow 1_{J+1}$
$R$ = universal gas constant divided by molecular weight, $m^2/sec^2K$
$S^*$ = coupling parameter, $cm^{-1}\,J^{-1}$
$S_0^*$ = unsaturated coupling parameter, $cm^{-1}J^{-1}$
$S_M^*$ = optimum coupling parameter, $cm^{-1}\,J^{-1}$
$T_0$ = translational temperature of gas mixture, $K$
$T_R$ = rotational temperature, K
$t$ = mirror transmittance
$t_m$ = mirror transmittance for maximum power output
$U'$ = macroscopic flow velocity, m/sec

Received December 18, 1972; revision received May 28, 1975. The authors wish to thank the technical editor and referee for their helpful comments. This work was supported by the Air Force Office of Scientific Research, Mechanics Branch, under Contract F 44620-71-C-0030-000002, and part was presented at the Ninth International Symposium on Rarefied Gas Dynamics, 1974, Göttingen, Germany. The authors also are grateful to R. Hanchett of Marc Analysis Research Corporation, Providence, R.I., for assistance in the numerical analyses.

Index category: Lasers.

*Research Assistant, Division of Engineering. Student Member AIAA.

†Division of Engineering; presently Assistant Professor, Department of Industrial Chemistry, Queen's University of Belfast, Belfast, Northern Ireland.

‡Professor, Division of Engineering.

$U$ = nondimensional macroscopic flow velocity, $U'/(2RT_0)^{1/2}$
$V$ = cavity volume, $m^3$
$W_M$ = cavity width for which laser intensity vanishes at the end of the cavity, meters
$x$ = coordinate along the cavity optical axis
$Z$ = convective time of the flow, $\equiv \tau z/U = z'/U'$, sec
$z'$ = distance measured in the flow direction, meters
$z$ = nondimensional distance along the flow, $z'/W_M$
$\alpha$ = characteristic rate constant for the problem, $sec^{-1}$ $torr^{-1}$
$\Delta\nu_D$ = Doppler width (full width at half maximum), $\equiv \nu_{2J1J+1}(2RT_0)^{1/2}(\ell n2)^{1/2}/c$, MHz
$\Delta\nu_H/2$ = collisional line width (full width at half maximum), MHz
$\epsilon_i$ = collisional half width for rotational level $i$
$\gamma_{cr}$ = $\gamma$ critical
$\zeta_{2J1J+1}$ = dimensionless frequency, $\equiv (\nu-\nu_{2J1J+1})(\ell n\,2)^{1/2}/\Delta\nu_D$
$\eta$ = nondimensional molecular velocity, $\equiv \xi/(2RT_0)^{1/2}$
$\eta_x, \eta_y, \eta_z$ = three components of nondimensional molecular velocity $\eta$
$\nu$ = frequency, MHz
$\nu_{2J1J+1}$ = frequency of lasing transition $2_J \leftrightarrow 1_{J+1}$ (10.6 $\mu$ for $CO_2$), MHz
$\xi$ = molecular velocity, m/sec
$\xi_x, \xi_y, \xi_z$ = three components of molecular velocity $\xi$, m/sec
$\sigma_i$ = elastic collision rate constant for vibrational level $i$, $sec^{-1}$ $torr^{-1}$
$\sigma_{ij}$ = elastic collision rate constant for $j$th rotational state of $i$th vibrational level, $sec^{-1}$ $torr^{-1}$
$\sigma_{ijx}$ = rotational relaxation rate constant for $j$th rotational state of $i$th vibrational level, $sec^{-1}$ $torr^{-1}$
$\tau$ = characteristic time of the flow, $\equiv W_M/(2RT_0)^{1/2}$, sec
$(2RT_0)^{1/2}$ = the velocity used to nondimensionalize various parameters in this manuscript, m/sec

## I. Introduction

MOLECULAR lasers utilizing high-speed flowing gases have come to be of increasing importance within recent years.[1] In particular, the $CO_2$-$N_2$ laser,[1-4] and other chemically excited lasers have shown promise of high gain coupled with high efficiency. It is the purpose of this study to examine the effects of inhomogeneous broadening and rotational relaxation upon various laser parameters such as power, gain, saturation intensity, and energy per unit cavity volume. Inhomogeneous broadening effects come into play as a consequence of the thermal motion of the gas molecules. It becomes necessary to distinguish between those molecules that can interact with the lasing radiation and those whose Doppler shift is too large to permit significant interaction. Consider, for example, a molecule whose upper and terminal lasing levels have, in the limit, a zero homogeneous line width. For this case, only particles with a zero component of velocity in the direction of a resonance photon will be able to participate in the processes of absorption or stimulated emission. Other particles with a component of velocity in the photon direction will be Doppler shifted and will 'see" a different frequency. These particles do not contribute to the stimulated emission, and there is zero power output. This occurs, as a consequence of "collisional hole filling" or velocity diffusion effects, at pressures of the order of a fraction of a torr for $CO_2$ lasers.

Only when homogeneous broadening dominates do all particles participate directly in the lasing process. One of the main purposes of this study will be to obtain a measure of the range of densities at which the assumption of homogeneous broadening (and the associated use of rate equations) is valid. Some $CO_2$ lasers operate in a region in which the ratio of homogeneous to inhomogeneous broadening is approximately one or larger, and chemical lasers may operate in regimes in which the power loss due to inhomogeneous broadening may become significant. For this reason, it is perhaps important to have a description of laser processes that encompasses the whole range of broadening and relaxation effects to determine the pressure dependence of laser performance characteristics. In order to proceed to such a goal, we must consider a description that properly accounts for the thermal motion of gas particles, relaxation phenomena associated with elastic collisions, as well as inelastic rotational and vibrational energy transfer. A laser theory using velocity-independent rate equations cannot do this, and it is necessary to formulate a kinetic theory involving particle distribution function and radiative effects. This is mandatory even through the mean free path, the usual criterion for the use of kinetic equations, may be small. Important partmeters that determine whether or not kinetic equations should be employed are given by the ratio of homogeneous to inhomogeneous broadening, $b$, the elastic collision cross section that determines the rate at which collisions will cause particles to diffuse (in velocity space) to fill the hole "burned" in the velocity distribution function of the upper lasing state, and the rate of rotational energy relaxation. Other studies[5-8] have utilized a modified rate equation formalism to examine these effects in lasers with zero flow, and it shall be our task in the following to assess inhomogeneous broadening effects, as well as elastic and rotational relaxation in a molecular gas flow laser system. In essence, this paper attempts to extend some previous results by Cool on gas flow lasers to include inhomogeneous broadening as well as additional relaxation effects.

## II. High-Speed Flow Laser

Figure 1 shows the physical model for the laser being studied. The flow is perpendicular to the lasing cavity. All excitation is assumed to occur upstream of the cavity, so that only relaxation effects occur in the cavity itself. This allows greater flexibility in the scaling of such devices since the nonlinear coupling between cavity gain and the excitation mechanism is removed. It is also apparent that such a system is more amenable to analysis. The flow in the cavity is one-dimensional and isothermal. In the proper limits our results reduce to those of Cool.

## III. Molecular Relaxation and Kinetic Equations

The general model for molecular relaxation is identical to that utilized by Cool[1] and others, and is illustrated in Fig. 2. A diatomic molecule, level 3, excited chemically, electrically, or by means of a flow expansion, is in resonance with the $CO_2$ upper lasing level 2. This is the pump source for the $CO_2$, and this molecule might be $N_2$ or a chemically excited hydrogen halide. The terminal lasing level of the $CO_2$ is in equilibrium with several nearby states. Only a small fraction of the particles in Group 1 is in the terminal lasing level. Further details and discussion of this model of the $CO_2$ laser excitation are presented in Ref. 1. Although the modeling here is with reference to the $CO_2$ laser system, the qualitative conclusions may be extrapolated to describe rotational relaxation effects and inhomogeneous broadening losses in chemical lasers where the reactions and inversion mechanisms may be more complex.

The necessity of using kinetic rather than rate equations has been discussed previously, and for atomic systems these equations have been discussed in detail elsewhere.[9-11] Here we will introduce an additional complication associated with

rotational energy transfer and relaxation. We assume that the population of states 0 and 4 (see Fig. 2) does not change significantly in the lasing cavity. Also, since quantities do not vary appreciably in a direction parallel to the lasing cavity, only variations in the flow direction will be considered. The variables may thus be considered to have been averaged over the direction of the laser cavity axis. Boundary-layer effects are neglected.

We considered vibration-rotation transitions between the upper and lower lasing level, as shown in Fig. 3, resonance collisional pumping of the upper state, and relaxation effects due to elastic collisions. Even for the simplified system in Fig. 2, this involves, in principal, a kinetic equation for each rotational level. It is clear that further simplifying assumptions are to be made. However, it should be noted that no assumption of a Boltmann distribution among the particles of the upper or terminal lasing states will be made.

We consider first the kinetic equation for the upper pumping state, 3.

$$\frac{(\eta_z+U)}{\tau}\frac{df_3}{dz}=K_{34}(M_{43}-f_3)$$
$$+K_{32}(M_{23}-f_3)+\sigma_3(M_{33}-f_3) \quad (1)$$

It is assumed that rate constants for resonance transfer are independent of rotational quantum numbers. The terms $K_{ij}$ $M_{ji}$ represent the source terms for an in elastic encounter between particles $i$ and $j$. It is assumed that these source terms have a Maxwellian velocity distribution, $M_{ij}$. By construction, $(K_{ij}/K_{ji})\int_{-\infty}^{\infty}M_{ji}\,d\xi=n_j$, the number of particles in vibrational state $j$. This assures that the first velocity moment of the kinetic equations will yield the usual rate equations for particle number density. The elastic collision rate constants, $\sigma_i$, are large. Equation (1) also assumes that the translational temperatures and macroscopic velocities of all species are identical.

We consider now the kinetic equations for the upper lasing state, $2_J$, and the terminal lasing state, $1_{J+1}$. These correspond to $P$ branch transitions.

$$\frac{(\eta_z+U)}{\tau}\frac{df_{2J}}{dz}=K_{2J3}\left[\left(\frac{\eta_{2J}}{\eta_2}\right)_{eqm}M_{32J}-f_{2J}\right]$$
$$+K_{2J1}\left[\left(\frac{\eta_{2J}}{\eta_2}\right)_{eqm}M_{12J}-f_{2J}\right]+\sigma_{2J}[M_{J2J}-f_{2J}]$$
$$+\sigma_{2Jx}\left[\left(\frac{\eta_{2J}}{\eta_2}\right)_{eqm}M_{22J}-f_{2J}\right]-4\pi A_{2J1J+1}f_{2J}$$
$$-A_{2J1J+1}Q_{2J1J+1}(f_{2J}-f_{1J+1}) \quad (2)$$

$$\frac{(\eta_z+U)}{\tau}\frac{df_{1J+1}}{dz}=$$
$$K_{1J+12}\left[\left(\frac{\eta_{1J+1}}{\eta_1}\right)_{eqm}M_{21J+1}-f_{1J+1}\right]$$
$$+K_{1J+10}\left[\left(\frac{\eta_{1J+1}}{\eta_1}\right)_{eqm}M_{01J+1}-f_{1J+1}\right]$$
$$+\sigma_{1J+1}[M_{1J+11J+1}-f_{1J+1}]+\sigma_{1J+1x}\left[\left(\frac{\eta_{1J+1}}{\eta_1}\right)_{eqm}\right.$$
$$\left.\times M_{11J+1}-f_{1J+1}\right]+4\pi(A_{2J1J+1}f_{2J}-A_{1J+10}f_{1J+1})$$
$$+A_{2J1J+1}Q_{2J1J+1}(f_{2J}-f_{1J+1}) \quad (3)$$

In Eqs. (2) and (3), the first two terms correspond, respectively, to changes in the $f_{2J}$ *and* $f_{1J+1}$ distribution functions as a consequence of vibrational excitation or de-excitation. The third terms represent changes in the velocity distribution function as a consequence of elastic thermalizing collisions that tend to remove radiation-induced anisotropies in the distribution function. The rate constant for this process is $\sigma_{2J}$ or $\sigma_{1J+1}$. The terms proportional to $\sigma_{2Jx}$ account for rotational energy exchange in a specific vibrational level. The fifth terms proportional to the Einstein coefficients, $A_{2J1J+1}$, $A_{1J+10}$ account for gain and loss due to spontaneous emission. In Eqs. (2) and (3), the $Q_{2J1J+1}$ term accounts for the effects of stimulated emission and absorption by selective interaction with particles in a certain range of the velocity spectrum. Thus it represents the number of photons per unit volume capable of being absorbed by a molecule in a given velocity range

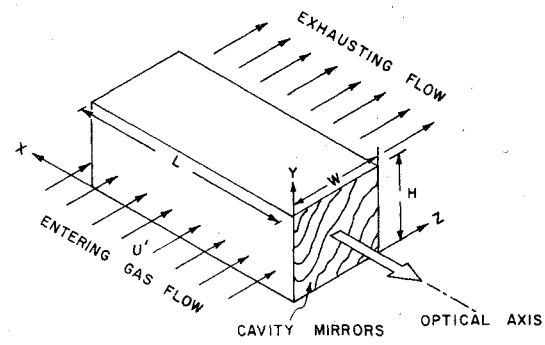


**Fig. 1 High-speed flow laser cavity description.**

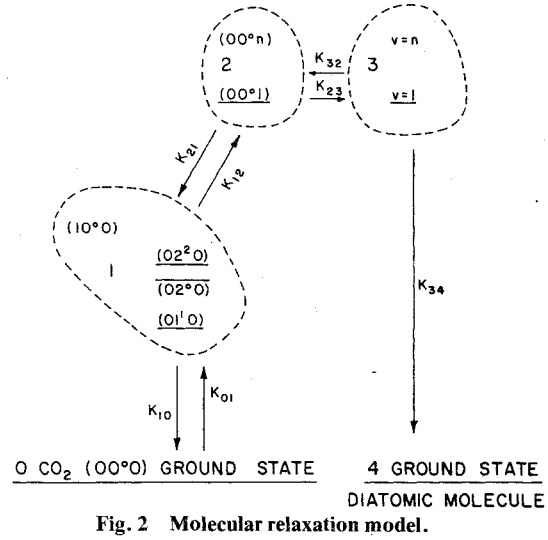


**Fig. 2 Molecular relaxation model.**

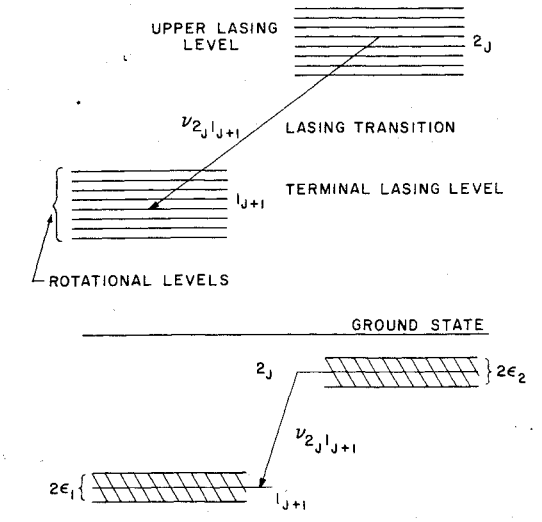


**Fig. 3 Details of collisional broadening of $2_J \leftrightarrow 1_{J+1}$ rotation-vibration transition.**

$$Q_{2JlJ+1}(f_\nu) = \int_{-\infty}^{\infty} d\zeta_{2JlJ+1} \int_{4\pi} d\Omega f_\nu \{\ell, (\upsilon - \upsilon_{2JlJ+1})\}$$

$$\times q_{2JlJ+1} \Delta\nu_D / (\ell n 2)^{1/2} \quad (4)$$

The line shape $q_{2JlJ+1}$, which should be Lorentzian in the rest frame of the molecule, is normalized such that

$$\int_{-\infty}^{\infty} q_{2JlJ+1} d\nu = 1 \quad (5)$$

It is assumed that $\nu_{2JlJ+1}$, the lasing frequency, is at a cavity resonance, and only one longitudinal mode is permitted to oscillate.

The steady-state equation of radiative transfer may be written as follows, assuming that only radiation in the $2_J - 1_{J+1}$ line is of importance.

$$\ell \cdot \frac{df_\nu}{dx} = \frac{A_{2JlJ+1} c^2}{2\nu_{2JlJ+1}^2} [H_{2l}(f_{2J}) + f_\nu H_{2l}(f_{2J} - f_{1J+1})] \quad (6)$$

The coupling of the kinetic equations occurs through the $Q_{2JlJ+1}$ and $H_{2l}$ terms. These are functionals of $f_\nu$, and $f_{2J}$ and $f_{1J+1}$, respectively. The number of particles, per unit volume, per unit solid angle about $\ell$ capable of absorbing a photon on a line centered about $\upsilon_{2Jl+1}$ is given by $H_{2l}(f_{1J+1})$, where by definition

$$H_{2l}(f_{2J} - f_{1J+1}) \equiv \int_{-\infty}^{\infty} (f_{2J} - f_{1J+1})\, q_{2JlJ+1} d\xi \quad (7)$$

In Eq. (6), the first term on the right-hand side represents spontaneous emission. For an intense lasing field, this term may be neglected for a rotation-vibration transition, and the gain may be immediately inferred to be

$$G(\zeta_{2JlJ+1}) = \frac{A_{2JlJ+1} c^2}{2\nu_{2JlJ+1}^2} H_{2l}(f_{2J} - f_{1J+1}) \quad (8)$$

Summing Eqs. (2) and (3) over $J$, we obtain equations for the velocity distribution functions $f_1$ and $f_2$ of particles in vibrational states 1 and 2. With the kinetic equations and the equation of radiative transfer, we may, in principle, solve for all quantities of interest.

## IV. Simplifying Assumptions

Subject to appropriate initial conditions at $z=0$, the equations developed previously are sufficient to obtain particle densities and photon intensity as a function of position and molecular and radiative parameters. The mathematical complexity introduced through the integral coupling terms $Q_{2JlJ+1}$ and $H_{2l}$ necessitates simplifications based on a plausible physical model.

Since all significant radiation will be in the lasing transition, it will be assumed that the photon distribution is given as follows:

$$f_\nu = L(z)\, H(z)\, \delta(\upsilon - \upsilon_{2JlJ+1}) \delta(l \pm \ell_x) \delta(\ell_y) \delta(\ell_z) \quad (9)$$

All photons propagate along the lasing axis, with a delta function in frequency. Upstream of $z=0$, there is no radiation intensity. Thus, only the lasing intensity must be obtained as a function of position. The Heaviside unit step function is represented by $H(z)$. The consequences of this assumption will be discussed in more detail when boundary conditions are considered.

In Fig. 4a, the Lorentzian line shape is shown. A further simplification is introduced whereby this is approximated by the spectrally flat profile, as illustrated in Fig. 4b.

In order that the spectrally flat profile match the line center results of the Lorentz profile in the limit of homogeneous broadening, it is necessary to keep the height as well as the half width of both profiles the same. The line shape function can then be written as follows:

$$q_{2JlJ+1}(\zeta_{2JlJ+1}) = \frac{H[b - (\zeta_{2JlJ+1} - \eta \cdot \ell)] H[b + (\zeta_{2JlJ+1} - \eta \cdot \ell)] (\ell n 2)^{1/2}}{\pi b \Delta\nu_D} \quad (10)$$

where

$$b \equiv \frac{(\epsilon_1 + \epsilon_2) c}{\nu_{2JlJ+1} (2RT_0)^{1/2}} = \frac{\Delta\nu_H (\ell n 2)^{1/2}}{2\, \Delta\nu_D}$$

dimensionless ratio of collisional line width to Doppler width.[10]

The collisional half widths, $\epsilon_1$ and $\epsilon_2$, are shown schematically in Fig. 3. We may assess the error introduced by this profile as follows. Were the velocity distribution function Maxwellian, then, from Eq. (8), the gain for a spectrally flat line shape is

$$G_{S.F} \sim \frac{(\ell n 2)^{1/2} \mathrm{erf}(b)}{\pi b \Delta\nu_D}$$

For a Lorentzian profile (in the molecule's rest frame) the gain is

$$G_L \sim \frac{(\ell n 2)^{1/2} e^{b^2} (1 - \mathrm{erf}(b))}{\Delta\nu_D \sqrt{\pi}}$$

taking the ratio of these two as a function of $b$, we find $(G_{SF}/G_L)_{b\to\infty} = 1$, $(G_{SF}/G_L)_{b=0} = 0.636$ and $(G_{SF}/G_L)_{b=1} \equiv 1.1$. Therefore, it seems reasonable to expect, at most, errors of the order of 30% with the introduction of the spectrally flat profile for very small values of $b$. For intermediate values, $b \sim 0(1)$, this error should be less. Calculations by Cabezas and Treat[12] indicate the effects of different line shapes on laser output.

Equation (10) allows the immediate calculation of $Q_{2JlJ+1}$ from Eq. (4) using the assumed photon distribution function (Eq. 9).

$$Q_{2JlJ+1} = \frac{2L(z) H(z) H[b - \eta_x] H[b + \eta_x] (\ell n 2)^{1/2}}{b \pi \Delta\nu_D} \quad (11)$$

Integrating Eqs. (1-3) over all velocity space yields, using Eq. (11), the rate equations. Assuming $K_{43} \approx K_{34} \approx 0$, the pumping

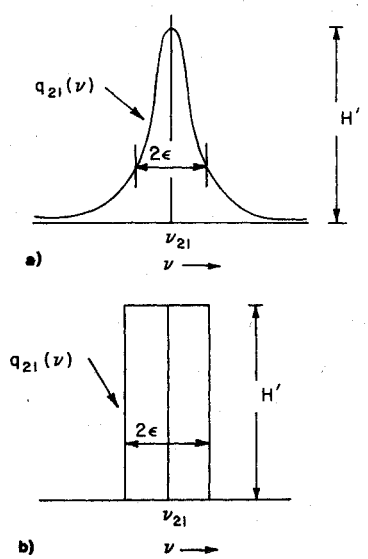


**Fig. 4 Collisional line shape: a) true, b) modeled.**

rate equation becomes

$$(U/\tau)\,(dn_3/dz) = K_{23}n_2 - K_{32}n_3 \tag{12}$$

The rate equation for the upper lasing level becomes

$$(U/\tau)\,(dn_{2J}/dz) = K_{32}Bn_3 + K_{12}Bn_1 + \sigma_{2Jx}Bn_2 - (K_{23} + K_{21} + \sigma_{2Jx} + 4\pi A_{2J1J+1})n_{2J} - \int_{-\infty}^{\infty} A_{2J1J+1}Q_{2J1J+1}(f_{2J} - f_{1J+1})\,d\xi \tag{13}$$

Summing this equation over all rotational states immediately yields the equation for the population in the "2" level vibrational state. It should be noted that the last term in the previous equation, corresponding to stimulated emission in the $2_J \rightarrow 1_{J+1}$ vibration-rotation line, is not summed. This is a consequence of the assumption that only one line is permitted to oscillate. Thus

$$\frac{U}{\tau}\frac{dn_2}{dz} = K_{32}n_3 + K_{12}n_1 - (K_{23} + K_{21} + 4\pi A_{21})n_2 - R(z) \tag{14}$$

where

$$R(z) = \int_{-\infty}^{\infty} A_{2J1J+1}Q_{2J1J+1}(f_{2J} - f_{1J+1})\,d\xi \tag{15}$$

Similarly, we obtain an equation for the particles in group 1. Thus, the kinetic equation for all particles in group 1 is given as

$$(U/\tau)\,(dn_1/dz) = (K_{21} - K_{01} + 4\pi A_{21})n_2 + (n_1 + n_2 + n_0)K_{01} - (K_{12} + K_{10} + K_{01} + 4\pi A_{10})n_1 + R(z) \tag{16}$$

These equations are essentially those used by Cool, with the following differences: finite rotational relaxation effects are present, no assumption of the ratio of $n_{2J}/n_2$ is made, and collisional relaxation effects are included. Only in the limit of the rotational relaxation parameter, $\sigma_{2Jx} \rightarrow \infty$, will $n_{2J}/n_2$ be given by the Boltzmann factor. Another important difference is that the stimulated emission terms depend upon integrals over the velocity distribution functions of the upper and terminal laser levels. Only those particles whose velocity is such that they are not Doppler shifted beyond

$$(b - \zeta_{2J1J+1}) < \eta_x < (b + \zeta_{2J1J+1}) \tag{17}$$

contribute directly to the gain in the assumption of a spectrally flat emission profile.

In obtaining the rate equations from the first moment of the kinetic equations, terms such as $(d/dz)\int_{-\infty}^{\infty}\eta_z(f_i/\tau)\,d\xi$ would normally appear. In this case they vanish because of the orthogonality of the radiation-induced anistropies and gradients in the flow direction.

At this point, an additional assumption will be made. Of the particles in group 1, only a small percentage is in the terminal lasing level. It will be assumed that conditions are far above threshold, and that $n_{1J+1} << n_{2J}$. This simplification will introduce an error of less than 10% when our results, in the proper limits, are compared with those of Cool. Therefore, there are five unknowns, $n_1$, $n_2$, $n_{2J}$, $n_3$, and $R(z)$. One additional equation must be obtained from the kinetic equation of $f_{2J}$ by taking the gain moment of Eq. (2). Operating on Eq. (2) with

$$\int_{-\infty}^{\infty} \frac{H[b - (\zeta_{2J1J+1} - \eta_x)]\,H[b + (\zeta_{2J1J+1} - \eta_x)]\,(\ell n2)^{1/2}}{\pi b \Delta\nu_D} \ldots d\xi$$

We obtain the following:

$$\frac{U}{\tau}\frac{d}{dz}H_{21}(f_{2J}, \zeta_{2J1J+1}) = \frac{\mathrm{erf}(b)\,(\ell n2)^{1/2}}{\pi b \Delta\nu_D}\,[K_{32}Bn_3 + K_{12}Bn_1 + \sigma_{2J}n_{2J} + \sigma_{2Jx}Bn_2] - H_{21}(f_{2J}, \zeta_{2J1J+1})\,[K_{23} + K_{21} + \sigma_{2J} + \sigma_{2Jx} + 4\pi A_{2J1J+1}] - \frac{2(\ell n2)A_{2J1J+1}L(z)H(z)}{\pi^2 b^2 \Delta\nu_D^2}\int_{-\infty}^{\infty}\{f_{21} - f_{1J+1})\,H[b - (\zeta_{2J1J+1} - \eta_x)]\,H[b + (\zeta_{2J1J+1} - \eta_x)]\,H[b - \eta_x]\,H[b + \eta_x]\}\,d\xi \tag{18}$$

The general moment of $H_{21}(f_{2J}, \zeta_{2J1J+1})$ does not close the system of equations. However, for $\zeta_{2J1J+1} = 0$, i.e., at line center, we note that as a consequence of the spectrally flat line shape $[H(x)]^2 = H(x)$, where $x$ is any argument of the Heaviside function. This results in a great mathematical simplification, the price for which is that detuning effects are excluded from the analysis.

Thus,

$$\frac{U}{\tau}\frac{d}{dz}H_{21}(f_{2J}, \zeta_{2J1J+1} = 0) = \frac{\mathrm{erf}(b)\,(\ell n2)^{1/2}}{\pi b \Delta\nu_D}\,[K_{32}Bn_3 + K_{12}Bn_1 + \sigma_{2J}n_{2J} + \sigma_{2Jx}Bn_2] - H_{21}(f_{2J}, \zeta_{2J1J+1} = 0) \times [K_{23} + K_{21} + \sigma_{2J} + \sigma_{2Jx} + 4\pi A_{2J1J+1} + \frac{2A_{2J1J+1}L(z)H(z)\,(\ell n2)^{1/2}}{b\pi\Delta\nu_D}] \tag{19}$$

In order for steady-state oscillation to occur in the cavity, it is necessary that gain be constant for constant losses and constant mirror transmittance. Consequently,

$$\frac{d}{dz}H_{21}(f_{2J}, \zeta_{2J1J+1} = 0) \propto \frac{d}{dz}G(f_{2J}, \zeta_{2J1J+1} = 0) = 0 \tag{20}$$

and

$$R(z) = \frac{4\nu_{2J1J+1}^2 L(z)H(z)G(\zeta_{2J1J+1} = 0)}{c^2} \tag{21}$$

or, in Cool's notation

$$R(z) = S^*I^* \qquad G(0) = S^*h\nu_{2J1J+1}$$

$$I^* = 4h\nu_{2J1J+1}^3 L(z)/c^2$$

Equations (19-21) may be combined to yield

$$R(z) = \mathrm{erf}(b)B(K_{32}n_3 + K_{21}n_1 + \sigma_{2Jx}n_2) + \mathrm{erf}(b)\sigma_{2J}n_{2J} - \frac{G(0)2\pi b\nu_{2J1J+1}^2\Delta\nu_D}{A_{2J1J+1}c^2\,(\ell n2)^{1/2}}\,[K_{23} + K_{21} + \sigma_{2Jx} + \sigma_{2J} + 4\pi A_{2J1J+1}] \tag{22}$$

and with $Z = \tau z/U$, the rate equations become

$$dn_3/dZ = K_{23}n_2 - K_{32}n_3 \tag{23}$$

$$d/n_2/dZ = K_{32}n_3 + K_{12}n_1 - (C' - \sigma_{2Jx})n_2 - R(Z) \tag{24}$$

$$dn_1/dZ = E'n_2 - Fn_1 + K_{01}(n_1 + n_2 + n_0) + R(Z) \tag{25}$$

$$dn_{2J}/dZ = K_{32}Bn_3 + K_{12}Bn_1 + \sigma_{2Jx}Bn_2 - C'n_{2J} - R(Z) \tag{26}$$

where $B$, $C'$, $E'$, and $F$ are listed in Appendix I. Equations (22-26) represent the essential physics of the effects of both homogeneous and inhomogeneous broadening, as well as collisional and rotational relaxation, subject to the restrictions previously mentioned. In the homogeneous broadening limit of $b\to\infty$, and thermally populated rotational states, $\sigma_{2Jx}\to\infty$, this formulation reduces to that of Ref. 1.

At this point, we may consider the behavior of the relaxation equations and the gain equation in the limit of homogeneous broadening. For the parameter $b\to\infty$, for fixed $\sigma_{2Jx}$ we have $G(0)\sim n_{2J}$; all particles in the $2_J$ state participate in the lasing process. Comparison of the gain equation for $R(Z)$ and the rate equation for $n_{2J}$ immediately informs us that $dn_{2J}/dZ=0$, for any value of the relaxation parameter. Since gain is constant in the cavity, and the upper lasing level (far above threshold) is proportional to the gain, $n_{2J}$ is fixed by cavity conditions. On the other hand, all of the other remaining upper nonlasing rotational levels are not necessarily constant in population as we proceed downstream.

Further information can be gained from a consideration of $\sigma_{2Jx}$. If we imagine that $\sigma_{2Jx}\approx 0$, i.e., no rotational energy transfer from neighboring rotational states, then $R(Z)$ is reduced by a Boltzmann factor when compared with the limit $\sigma_{2Jx}\to\infty$. In this latter limit, all rotational levels rapidly feed energy into neighboring states, so that the upper lasing level tends to become replenished by rotational transfer as it is depleted by stimulated emission. For the case of $\sigma_{2Jx}\to\infty$, to balance terms in the gain equation, we have

$$Bn_2=\frac{G(0)2\pi b\nu^2_{2J1J+1}\Delta\nu_D}{A_{2J1J+1}c^2(\ell n2)^{1/2}}$$

and $n_2=$ const. But for this homogeneously broadened limit, we find from Eq. (8)

$$n_{2J}=\frac{G(0)2\pi b\nu^2_{2J1J+1}\Delta\nu_D}{A_{2J1J+1}c^2(\ell n2)^{1/2}}$$

Consequently, we have a Boltzmann distribution, $n_{2J}/n_2=B$. Substituting this into Eq. (24), and using the fact that $n_2=$ const for $b\to\infty$, the stimulated emission term becomes,

$$R(Z)=K_{32}n_3+K_{12}n_1-\frac{G(0)2\pi b\nu^2_{2J1J+1}\Delta\nu_D}{A_{2J1J+1}c^2(\ell n2)^{1/2}B}[K_{23}+K_{21}+4\pi A_{21}]$$

which, when compared with the equation for $\sigma_{2Jx}\to 0$, is larger by a Boltzmann factor. As $\sigma_{2Jx}$ increases, all states can indirectly participate in the lasing process by feeding the $2_J$ state that is depopulated by stimulated emission.

## V. Boundary Conditions

We consider the state of the gas at the entrance to the lasing cavity as known, and our task is to find the initial conditions on the gas immediately inside the cavity in terms of these upstream conditions. As noted, our analysis is restricted to plane waves within the cavity, subject to the condition that saturated gain must equal the losses at line center. Consequently, there will be an initial burst of radiation in order that this condition be met. This rapid relaxation to meet cavity conditions occurs on the order of the photon transit time in the cavity, and the width of this zone is this photon transit time $t_p\sim 10^{-8}$ sec multiplied by $U'$, the macroscopic flow velocity. This width is assumed to be much less than any quantity of interest in the problem, although in reality, it can be of the order of a rotational relaxation length. It should also be mentioned that this initial spike of radiation is not physically observed, and is doubtlessly a consequence of the assumption of plane waves and the attendant neglect of diffraction effects. Once inside the cavity, the actual situation should be sufficiently well approximated by a plane wave assumption.

Using $-$ and $+$ to denote conditions upstream and downstream of the initial discontinuity, we note the following conditions. The diatomic pumping molecules play no role in the radiative discontinuity, and

$$n_3^-=n_3^+ \tag{27}$$

Furthermore, only rotational relaxation and stimulated emission occur across the entrance. Therefore,

$$n_1^-+n_2^-=n_1^++n_2^+ \tag{28}$$

To assess the effect of the jump conditions on the density of the upper lasing state, it is necessary to solve Eq. (8) for $f_{2J}$ subject to the conditions that as $b\to 0$, no particle can interact with the lasing radiation. As $b\to\infty$ all particles can participate, and $f_{2J}$ will saturate uniformly, independent of velocity. Thus,

$$f^+_{2J}=n^-_{2J}\{1-H[b-\eta_x]H[b+\eta_x]\}\left[\frac{1}{2\pi RT_0}\right]^{3/2}e^{-\eta^2}+\left\{\frac{G(0)2\pi b\nu^2_{2J1J+1}\Delta\nu_D}{A_{2J1J+1}c^2(\ell n2)^{1/2}}\;\frac{H[b-\eta_x]H[b+\eta_x]\sqrt{\pi}}{2b}\right\}\times\left[\frac{1}{2\pi RT_0}\right]^{3/2}\exp(-\eta_y^2-\eta_z^2) \tag{29}$$

Integrating this expression with respect to velocity, we obtain

$$n^+_{2J}=(1-\mathrm{erf}(b))n^-_{2J}+\frac{G^+(0)2\pi b\nu^2_{2J1J+1}\Delta\nu_D}{A_{2J1J+1}c^2(\ell n2)^{1/2}} \tag{30}$$

Subtracting Eq. (26) from Eq. (24), and neglecting vibrational relaxation across the discontinuity yields

$$dn_{2x}/dZ\simeq-\sigma_{2Jx}Bn_{2x}+\sigma_{2Jx}(1-B)n_{2J} \tag{31}$$

Using Eq. (30) for $n^+_{2J}$, we obtain

$$n^+_{2x}=\{1-\mathrm{erf}(b)\}n^-_{2x}+\mathrm{erf}(b)n^-_{2x}\exp[-\sigma_{2Jx}BZ]+\frac{G^+(0)2\pi b\nu^2_{2J1J+1}\Delta\nu_D}{A_{2J1J+1}c^2(\ell n2)^{1/2}}\left[\frac{n_{2x}}{n_{2J}}\right]_{\mathrm{eqm}}[1-\exp(-\sigma_{2Jx}BZ)] \tag{32}$$

In the limit of no rotational relaxation within the initial discontinuity, $\sigma_{2Jx}BZ<<1$ and we find that

$$n^+_{2x}=n^-_{2x} \tag{33}$$

Our boundary conditions on $n^+_{2J}$, $n^+_1$, $n^+_2$, $n^+_3$ are now determined in terms of known upstream conditions and known parameters. Cool's boundary conditions correspond to $b\to\infty$ and $\sigma_{2Jx}\to\infty$. Thus, From Eq. (32) we obtain

$$n^+_{2x}=\left[\frac{n_{2x}}{n_{2J}}\right]_{\mathrm{eqm}}\left[\frac{G^+(0)2\pi b\nu^2_{2J1J+1}\Delta\nu_D}{A_{2J1J+1}c^2(\ell n2)^{1/2}}\right]=\left[\frac{n_{2x}}{n_{2J}}\right]_{\mathrm{eqm}}n^+_{2J}$$

which is a Boltzmann distribution for the rotational levels.

## VI. Solution of the Equations, Spatially Homogenous Limit

We now have four first-order linear differential equations for $n_1$, $n_2$, $n_{2J}$, and $n_3$, and an algebraic expression for $R(Z)$ given in terms of these unknowns and the radiative parameters. The boundary conditions within the cavity at $Z=0^+$ are also known in terms of given upstream ($0^-$) en-

trance conditions. These equations can be reduced to a fourth-order differential equation of the form,

$$R^{IV}(Z)+\gamma_1 R'''(Z)+\gamma_2 R''(Z)+\gamma_3 R'(Z)$$
$$+\gamma_4 R(Z)+\alpha_{41}+\alpha_{42}=0 \tag{34}$$

where $\gamma_1$, $\gamma_2$, $\gamma_3$, $\gamma_4$, $\alpha_{41}$, and $\alpha_{42}$, are constants independent of $Z$ and are given in Appendix 1. The solution of these equations takes the form

$$R(Z)=\left[\sum_{i=1}^{4}\beta_{i1}\exp(m_i Z)-\frac{\alpha_{41}}{\gamma_4}\right]$$
$$-\frac{G(0)}{h\nu_{2J1J+1}}\left\{\sum_{i=1}^{4}\beta_{i2}\exp(m_i Z)+\frac{\alpha'_{42}}{\gamma_4}\right\} \tag{35}$$

The $m_i$ are the roots of the quartic

$$m^4+\gamma_1 m^3+\gamma_2 m^2+\gamma_3 m+\gamma_4=0 \tag{36}$$

Initial conditions on the derivatives of $R(Z)$ are obtained by repeated differentiation of Eqs. (22-26), and these determine the coefficients $\beta_{ij}$. From Eq. (35) we may define, as in Ref. 1, the local saturation parameter ($I_s^*$) at a given position along the flow as

$$I_s^*=\beta_{12}e^{m_1 Z}+\beta_{22}e^{m_2 Z}+\beta_{32}e^{m_3 Z}+\beta_{42}e^{m_4 Z}+\alpha'_{42}/\gamma_4) \tag{37}$$

Algebraic results for certain limiting cases have been obtained, and in the proper limit the results reduce essentially to those of Cool. They are too lengthy to be presented here, and we shall illustrate a typical case numerically in Sec. VII.

The cavity oscillation conditions are identical to those of Cool and will not be reproduced here. The power output is given by integrating $R(Z)$ along the cavity width, and

$$P=\frac{h\nu_{2J1J+1}U'V}{W_M}\int_0^{W_M/U'}\frac{t}{a+t}R(Z)\,dZ \tag{38}$$

Maximum power output may be obtained by setting $\partial P/\partial t=0$. Following Cool,

$$P_{\max}=\frac{HU't_m^2}{a(1-a-t_m)}\int_0^{W_M/U'}I_s^*\,dZ \tag{39}$$

$$t_m=a\left[\frac{1-a-t_m}{a+t_m}\right]\left[\{h\nu_{2J1J+1}L\int_0^{W_M/U'}S_0^*I_s^*dZ/\right.$$
$$\left.\int_0^{W_M/U'}I_s^*dZ\}+\ell n(1-a-t_m)\right] \tag{40}$$

The width at which intensity vanishes is given by $W_M$. An optimum coupling parameter, or gain, is defined as follows:

$$S_M^*=-\ell n(1-a-t_m)/h\nu_{2J1J+1}L \tag{41}$$

This assures that the cavity length is such that the intensity goes to zero at the cavity exit.

The effects of $\sigma_{2Jx}$ has been discussed for the limiting case of homogeneous broadening. For inhomogeneous broadening, it will be necessary to consider numerical results. First, however, it is perhaps of interest to examine the spatially homogeneous limit. For this case, we obtain the following from Eq. (34):

$$R(Z=\text{const})=-(\alpha_{41}+\alpha_{42})/\gamma_4 \tag{42}$$

To assess the pressure dependence of unsaturated gain and the local saturation parameter, we must make certain assumptions on the dependence of the excitation level on pressure. With Cool, we assume that this excitation ratio $n_{2J}/n_0$ is independent of pressure, so as we double pressure at the cavity inlet, we double the number of particles in the upper lasing state. The $K_{ij}$, $n_i$, and $b$ all vary linearly with pressure. In Cool's notation, Eq. (42) can be rearranged as

$$S^*=S_0^*/(1+I^*/I_s^*) \tag{43}$$

where

$$S_0^*=-\alpha_{41}/\alpha'_{42} \tag{44}$$

and

$$I_s^*=\alpha'_{42}/\gamma_4 \tag{45}$$

From Eq. (43), we see that the saturation dependence of gain is that of homogeneous broadening, with a Lorentz cross section in the rest frame of the atom. It should be noted that this is also the form of the saturation for inhomogeneous broadening if the assumption of a spectrally flat profile is made. This is, as noted, a necessary assumption for closure of the equations and permits a solution to be obtained without having to solve for the velocity distribution function. We can now consider the pressure behavior of unsaturated gain. From Eq. (44) we find

$$S_0^*\sim \text{erf}\,(b)\,.$$

Thus for small $b$, unsaturated gain is proportional to pressure, and for large $b$, it is independent of pressure. At values of $b\geq 1$ the unsaturated gain is essentially homogeneously broadened. From Eq. (45) we obtain the pressure behavior of the local saturation parameter $I_s^*$ as

$$I_s^*\simeq p^2/(\text{erf}(b)\,(K_1/K_2)+1)$$

where $K_1$ and $K_2$ are constants independent of pressure. Thus for homogeneous broadening ($b\to\infty$), $I_s^*\sim p^2$. However, for inhomogeneous broadening there are two regimes. Because of the large rate constants for elastic collsions and rotational relaxation, we find that $K_1>>K_2$. Thus, even for $b\lesssim 1$ we still have erf $(b)$ $K_1>>K_2$. Consequently $I_s^*\sim p$. As pressure decreases, the erf $(b)$ decreases. For very low pressures erf $(b)$ $K_1<<K_2$ and $I_s^*$ again varies as $p^2$. A measure of the extent of these two regimes of inhomogeneous broadening can be associated with the following parameter

$$\gamma_{cr}=\frac{\text{erf}(b)K_1}{K_2}\simeq\text{erf}(b)\left[\frac{\sigma_{2J}}{\sigma_{2Jx}}+\frac{B(\sigma_{2J}+\sigma_{2Jx})}{K_{2l}+4\pi A_{2J1J+1}}\right]$$

and since

$$\frac{\sigma_{2J}}{\sigma_{2Jx}}\sim 0(1),\qquad \gamma_{cr}\simeq\frac{\text{erf}(b)B(\sigma_{2J}+\sigma_{2Jx})}{K_{2l}}$$

For $\gamma_{cr}>>1$ and $b<<1$, we have $I_s^*\sim p$, for $\gamma_{cr}<<1$, $I_s^*\sim p^2$. For $CO_2$ lasers, the ratio $B(\sigma_{2J}+\sigma_{2Jx})/K_{2l}$ is pressure independent but is of the order of $10^3$. Thus we see that velocity changing collisions and inelastic rotational level changing collisions are very important in determining the saturation characteristics of molecular lasers.

Let us now consider the dependence of maximum power ($P$) on pressure ($p$). If this power is proportional to the product of saturation intensity and gain, we obtain

$$P/Ap^2\sim\text{erf}(b)/(\gamma_{cr}+1)$$

For $\gamma_{cr}<<1$, the saturation behavior of $P/Ap^2$ is erf $(b)$. However, for $\gamma_{cr}>>1$, $P/Ap^2$ is independent of $b$. Since $K_1/K_2$ is large for $CO_2$, $b$ can be quite small, and $\gamma_{cr}$ can still be

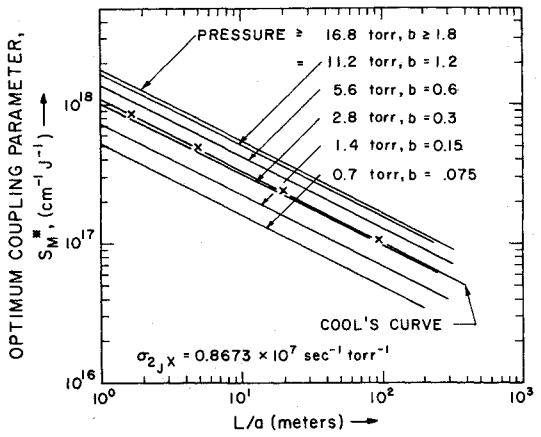


**Fig. 5 The optimum coupling parameter vs length divided by the cavity loss for $a = 0.04$.**

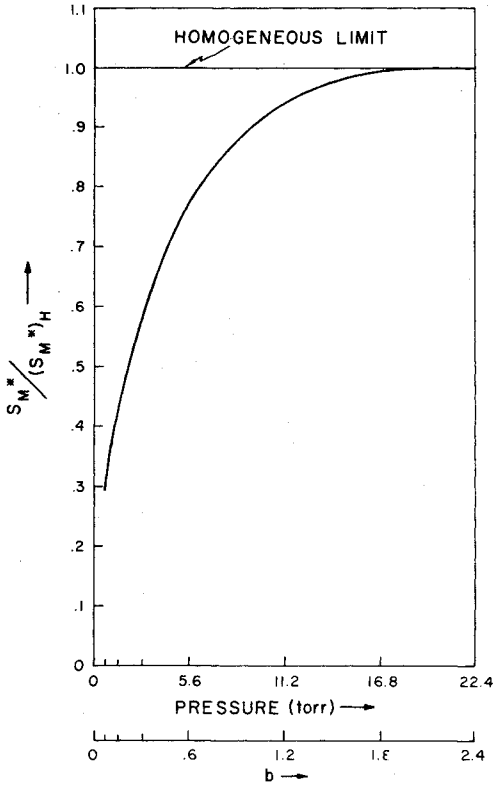


**Fig. 6 The optimum coupling parameter normalized by the value of the proper homogeneously broadened limit ($b \to \infty$) vs pressure.**

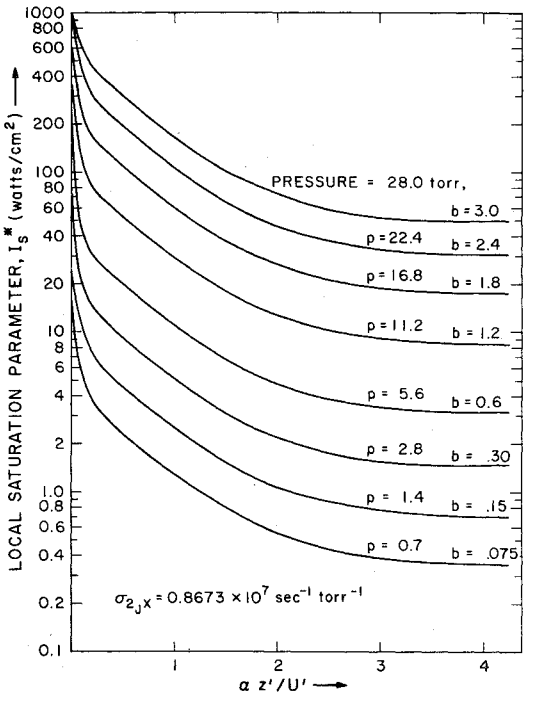


**Fig. 7 The local saturation parameter as a function of nondimensional distance along the flow for various values of $b$.**

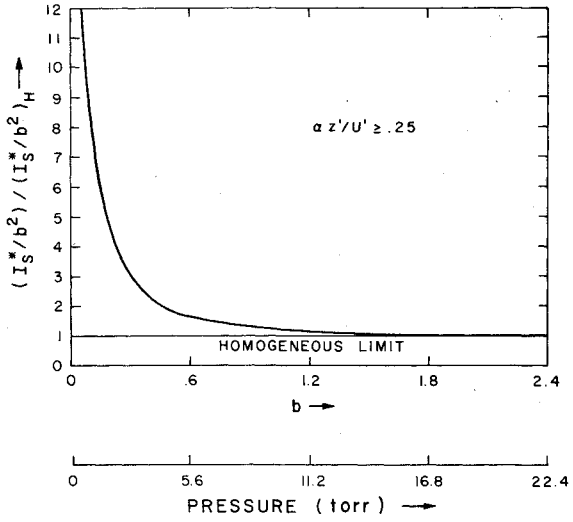


**Fig. 8 Pressure dependence of the local saturation parameter for $\alpha z'/U' \geq 0.25$.**

large. Thus, collisional effects extend homogeneously broadened behavior for power/area to quite low values of $b$ as a consequence of compensating effects in gain and saturation intensity.

## VII. Numerical Results

In order to compare our results for the general case of broadening with those of Cool for the homogeneously broadened limit, numerical results are presented for the parameters in Appendix II. First, however, it will be necessary to obtain from Cool's parameters his effective value of $b$. From Eqs. (8), we may calculate his value of gain for the homogeneously broadened limit, and $\sigma_{2J\,x} \to \infty$, without the knowledge of the form of the distribution function. This is given as

$$G(0) = \frac{A_{2_J1_{J+1}} c^2 (\ell n 2)^{1/2}}{2\pi b \nu_{2_J1_{J+1}}^2 \Delta\nu_D} \left[ \left[ \frac{n_{2_J}}{n_2} \right]_{\text{eqm}} n_2 - a_J \left[ \frac{n_{1_{J+1}}}{n_1} \right]_{\text{eqm}} n_1 \right]$$

where $a_J$ (which corresponds to Cool's $f_J$) is given in Appendix II. Using the parameters of Appendix II, we find that the value of $b$ is 1.22. From Ref. 13, for 5.6 torr, the value of $b$ should be slightly greater than 1. However, more recent experiments[14-15] seem to indicate that $b \approx 0.6$ at 5.6 torr, and it is this value that will be used in our calculations. The Doppler broadening for $CO_2$ at 300K is 53 MHz. From the cross sections and molecular weights, to within about 10%, this number is independent of composition for arbitrary mixtures of $CO_2$, $N_2$, and He. The other parameters that appear in addition to those in Cool's paper are $\sigma_{2J}$, the rate constant for elastic collisions responsible for the "hole filling" effect, and $\sigma_{2Jx}$, the rate constant for rotational relaxation. The elastic rate constant has been obtained from viscosity information on the constituent gases and a computer program based on the extended law of corresponding states has been used to obtain the value of the mixture.[18] The rotational relaxation constant is obtained from information in Refs. 16 and 17, and the

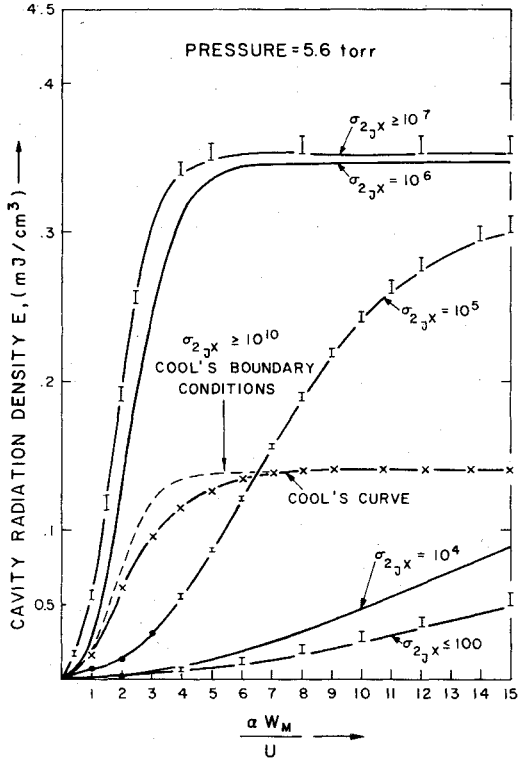


**Fig. 9 Variation of energy density per unit cavity volume with the maximum effective nondimensional cavity width. For a particular $\sigma_{2Jx}$(sec$^{-1}$), at 5.6 torr the error bars indicate the variation of $E$ when only $b$ is changed as a parameter ($0.075 \leq b \leq 3.0$).**

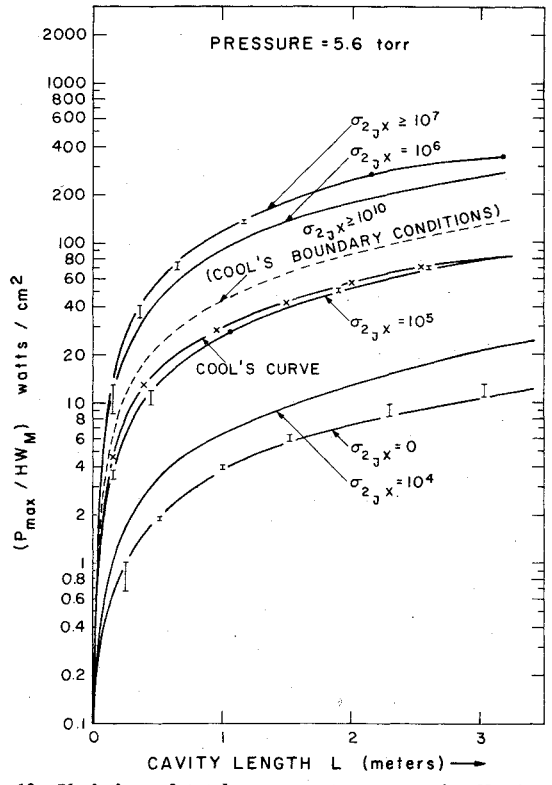


**Fig. 10 Variation of total power output per unit effective cavity cross-sectional area vs cavity length ($a = 0.04$). For a particular value of $\sigma_{2Jx}$(sec$^{-1}$), the error bars indicate variation of $P_{max}/HW_M$ as $b$(and hence pressure) is changed, when these curves have been rescaled by the square of the pressure so as to obtain all the curves at 5.6 torr.**

values for $\sigma_{2J}$ and $\sigma_{2Jx}$ are $0.7924 \times 10^7$ sec$^{-1}$ torr$^{-1}$ and $0.8673 \times 10^7$ sec$^{-1}$ torr$^{-1}$, respectively.

In our numerical results, one root of Eq. (36) was obtained to a high degree of accuracy using Newton's method, and the remaining roots were obtained by solution of the resulting cubic equation. As a consequence of the small difference of two large numbers appearing in the exponents, it was necessary to use double precision on a CDC 6600 in order to obtain stable results.

In Fig. 5 we see the optimum coupling parameter as a function of $L/a$, the length divided by the cavity loss. The parameters of Appendix II have been used to illustrate and compare with the results of Cool. The discrepancy between Cool's curve and our homogeneous limit is due largely to a more correct value of $b$. We clearly see the effect of $b$ in reducing the optimum coupling parameter, i.e., the optimum gain. We should note that the value of $b$ is chosen corresponding to that of $CO_2$, and that as $b$ is varied, we are actually varying pressure. Thus, $b=0.6$ as noted above, corresponds to 5.6 torr, $b=0.3$ corresponds to 2.8 torr, etc. It is assumed that as pressure changes, the initial excitation ratio, $n_{2J}/n_0$, remains constant. To within an accuracy of less than 4%, it is seen in Fig. 6 that this optimum coupling parameter, normalized by the value of the proper homogeneously broadened limit ($b \to \infty$) is independent of length. The gain decreases significantly for small $b$ and, indeed, is proportional to $b$ or pressure in the inhomogeneously broadened limit. As noted, this does not have the serious consequences for power output that we initially might have suspected, at least for the case of optimum width due to compensating factors in the product of gain and intensity. In Fig. 7 we see the saturation intensity as a function of $\alpha z'/U'$ and $b$. There is no asymptote, and the saturation intensity increases with $b^2$ for $b \gtrsim 2$. These results are well known. A more concise illustration of the pressure dependence of the saturation intensity is shown in Fig. 8, where $(I_s^*/b^2)_H$ denotes a value of $I_s^*$ for a given $b$, for $b>2$. Only for values of $b \lesssim 1$ do inhomogeneous broadening effects become prominent.

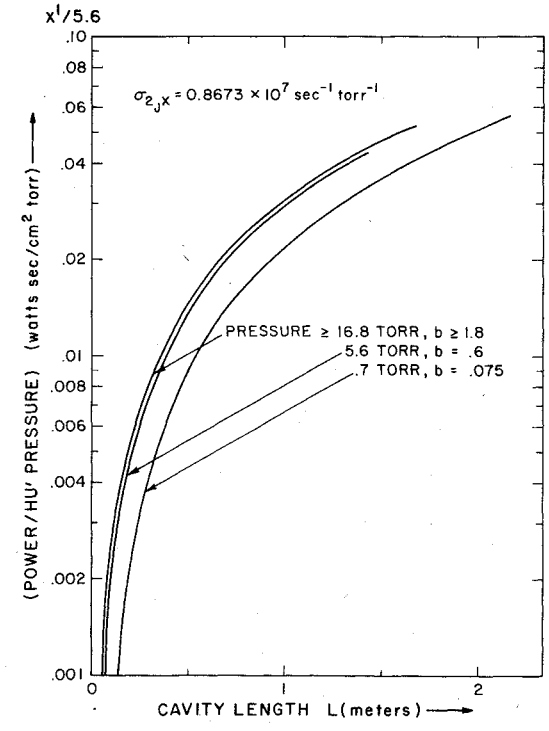


**Fig. 11 Total power output divided by cavity height, macroscopic flow velocity and pressure as a function of length ($a = 0.04$).**

The energy density per unit cavity volume may be defined as follows:

$$E = h\nu_{2J1J+1} \int_0^{W_M/U'} R(Z)\, dZ$$

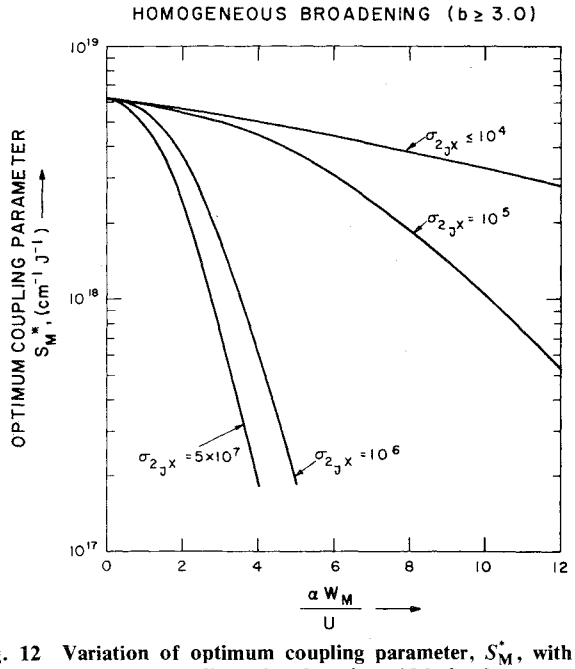


**Fig. 12 Variation of optimum coupling parameter, $S_M^*$, with the maximum effective nondimensional cavity width for homogeneous broadening ($b \geq 3.0$), $\sigma_{2Jx}$(sec$^{-1}$) is varied as a parameter. Pressure = 5.6 torr.**

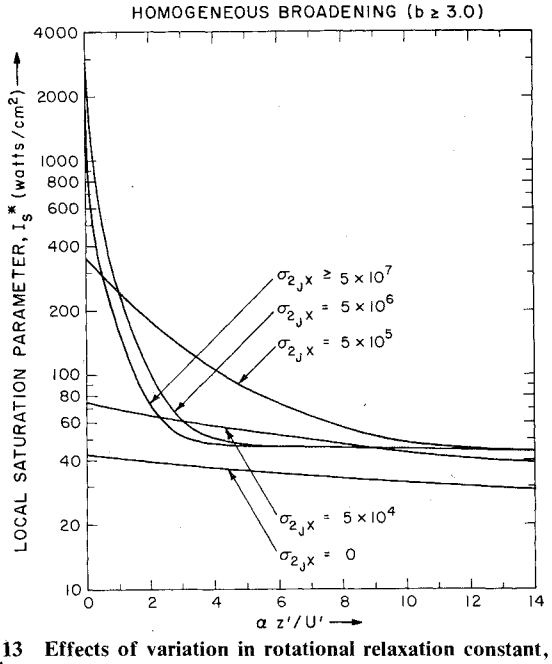


**Fig. 13 Effects of variation in rotational relaxation constant, $\sigma_{2Jx}$ (sec$^{-1}$), on local saturation parameter for homogeneous broadening ($b \geq 3.0$) and pressure = 28.0 torr.**

These results are shown in Fig. 9. For the values of Appendix II, $p = 5.6$ torr, if we imagine that $b$ is a variable parameter, there is less than 5% variation in energy density until pressure is of the order of a few tenths of a torr. For pressures above this level, as noted in the qualitative estimates of Eq. (34), there are practically no inhomogeneous effects. This is a consequence of the "diffusional" hole filling cited by T. Kan and G. Wolga.[19]

More important variations occur as a consequence of finite rotational relaxation rates. In Fig. 9 we see that for $\sigma_{2Jx} > 10^7$ sec$^{-1}$ at 5.6 torr, the relaxation is almost fast enough so that all levels contribute indirectly to the lasing intensity. The calculations here regard $\sigma_{2Jx}$ as a variable parameter. Values of $\sigma_{2Jx}$ lower than $\approx 10^6$ sec$^{-1}$ are perhaps unphysical, since rotational relaxation is always quite rapid but there can be even a noticeable power loss for $\sigma_{2Jx} \approx 10^6$ sec$^{-1}$, which is only three orders of magnitude faster than vibrational relaxation. These curves are calculated for the boundary conditions that do not allow rotational relaxation in the initial discontinuity. These boundary conditions, as discussed above, differ from those of Cool. In Fig. 9, for comparison's sake, Cool's boundary conditions are used for $\sigma_{2Jx} \to \infty$, and our numerical results are compared with his. The slight difference is largely a consequence of our neglect of the particles in the $1_{J+1}$ state of the lower lasing level.

In Fig. 10 we see the power output per unit area as calculated from Eqs. (39) and (40). For the normalization of the ordinate of Fig. 10, there is no additional influence of inhomogeneous broadening until, again, pressure becomes of the order of a few tenths of a torr. Until this lower limit, the $P_{\max}/W_M H$ is proportional to pressure squared. The effects of reducing the rate of rotational relaxation is significant as the relaxation shifts from an equilibrium ($\sigma_{2Jx} \to \infty$) value to a frozen ($\sigma_{2Jx} \to 0$) value. For comparison, the results of Cool's curve and our calculations with his boundary conditions are shown. The discrepancy between our numerical result and those obtained by Cool occur largely as a consequence of approximations made in the solution of Eq. (34), Ref. 1.

Although Fig. 10 shows essentially no $b$ dependence beyond that of the $p^2$ behavior of power, $W_M$ is dependent upon the value of $b$ for a given length, so that total power does vary with $b$. In Fig. 11 we see this effect on total power output. The additional reduction in total power (as a consequence of an increase in $W_M$) becomes significant for lower pressure.

Finally, in Figs. 12 and 13 again for the parameters of Appendix II, we see the effects of changing the rotational relaxation on $I_s^*$ and $S_M^*$. Decreasing $\sigma_{eJx}$ slows the rate at which energy can flow from rotational levels to the upper lasing level. In Fig. 13, although it is not evident with the abcissa scale used, $I_S^*(\sigma_{2Jx} = 5\times10^6, Z=0)/I_S^*(\sigma_{2Jx} = 5\times10^7, Z=0) << 1$.

## VIII. Conclusions

An attempt has been made to study the effects of inhomogeneous broadening and rotational relaxation on a general class of gas flow molecular lasers. A kinetic rather than rate equation approach was used to account properly for particle motion and velocity changing elastic collisions that fill the hole "burned" in the velocity distribution function of the upper lasing level. The Lorentz line profile (in the rest frame of the absorbing or emitting molecule) was approximated by a spectrally flat line shape. The radiation within the cavity has been assumed to consist of uniform plane waves. Only those systems are considered for which the initial excitation processes are uncoupled from the subsequent relaxation processes. We may draw the following conclusions.

1) The total power output is directly proportional to the flow velocity $U'$ and height $H$.

2) Total power output per unit effective cavity cross-sectional area for a given length of cavity for a $CO_2$ laser varies approximately (within 5%) as the square of the operating pressure for $b \geq .075$ and for rotational relaxation parameter, $\sigma_{2Jx} \geq 10^7$ sec$^{-1}$ (at 5.6 torr). The gas temperature and composition are assumed to be fixed and the same initial percentage of excited molecules are to be maintained for different pressures. The important parameter that determines power loss due to inhomogeneous broadening is not erf($b$) but erf ($b$) $B\ (\sigma_{2J} + \sigma_{2Jx})/K_{2J} \simeq \gamma_{cr}$. If $\gamma_{cr} >> 1$ the power per unit area decreases as pressure squared, whereas if $\gamma_{cr} << 1$ it will decrease more sharply, approximately as the cube of pressure.

3) Decreasing the rotational relaxation parameter, $\sigma_{2Jx}$ decreases laser power output, as excited molecules in the upper vibrational level of $CO_2$ remain confined to rotational levels other than upper lasing level and we have a non-

Boltzmann distribution. For $\sigma_{2Jx} \geq 10^7$ sec$^{-1}$ (at 5.6 torr), complete rotational equilibrium can be assumed to yield a Boltzmann distribution.

4) Subject to the conditions of (2), the total power output is directly proportional to pressure for $b \geq 0.6$. For $b << 0.6$, depending upon the length, power decreases sharply as a consequence of additional inhomogeneous broadening effects. Power exhibits a pressure dependence different from that of power per unit are since the optimum width is pressure dependent.

5) The local transmitted power output and the local saturation parameter start at very high initial values (at $Z = 0^+$) and decay exponentially in a four-stage relaxation process. For inhomogeneous broadening the initial stage is characterized by a time constant associated with the elastic collisions and rotational relaxation that tend to fill the hole "burned" in the velocity distribution function of the upper laser level. The time constant is approximately (erf $(b)$ $\sigma_{2J} + \sigma_{2Jx})^{-1}$. This relaxation stage is absent for homogeneous broadening. The next three stages occur for both homogeneous as well as inhomogeneous broadening. For inhomogeneous broadening the second stage is dominated by rotational relaxation, though both elastic velocity-changing and inelastic rotational level-changing collision processes replenish the upper laser level. This replenishment for molecular system with rotational fine structure takes place via successive collisions that change both rotational quantum numbers and velocities such that radiative interaction is enhanced. For $\sigma_{2Jx} \to 0$, the numerical results indicate that the time constant for this stage is essentially independent of $\sigma_{2J}$, whereas for any $\sigma_{2Jx}$, the time constant depends on both $\sigma_{2J}$ and $\sigma_{2Jx}$. For homogeneous broadening the elastic collisions are unimportant and the time constant for this stage is approximately $[\sigma_{2Jx} B]^{-1}$.

The third stage is characterized by a time constant $(\tau)$ associated with the rate of $(V \to V)$ transfer of energy to the upper laser level from the vibrationally excited diatomic molecules. This time constant is dependent upon $\sigma_{2Jx}$. For $\sigma_{2Jx} \geq 10^7$ sec$^{-1}$ (at 5.6 torr), $\tau \approx (K_{32})^{-1}$ whereas for $\sigma_{2Jx} \to 0$, $\tau \approx (BK_{32})^{-1}$. Thus the time constant differs by a Boltzmann factor, which is not surprising.

The fourth stage overlaps the third and has a time constant $(\tau)$ characterized by the relaxation rate of level 1 to the ground state by $(V-T)$ energy transfer processes. This time constant $\{\tau \approx (K_{10} + K_{01})^{-1}\}$ is independent of $\sigma_{2Jx}$.

6) The local saturation parameter varies as the square of the pressure for $b \geq 1.2$ and pressures $\geq 6.0$ torr. There is an intermediate region for $0.001 \leq b \leq 0.6$ where the local saturation parameter varies as pressure. For very small values of $b$ it again is proportional to the square of pressure. The parameter that determines the extent of the latter two regimes is $\gamma_{cr} \sim$ erf $(b)$ $B$ $(\sigma_{2J} + \sigma_{2Jx})$ $/K_{21}$. For inhomogeneous broadening, if $\gamma_{cr} >> 1$, $b << 1$, the saturation parameter varies linearly with pressure, whereas if $\gamma_{cr} << 1$, the saturation parameter is proportional to the square of the pressure.

## Appendix I

$$\left[\frac{n_{2J}}{n_2}\right]_{eqm} \equiv B = g_J \frac{2hcB''}{kT_R} \exp\left\{-\frac{hcB''}{kT_R} J(J+1)\right\}$$

$$\left[\frac{n_{1J+1}}{n_1}\right]_{eqm} \equiv B_1 = g_{J+1} \frac{2hcB'}{kT_R} \times \exp\left\{-\frac{hcB'}{kT_R}(J+1)(J+2)\right\}$$

where

$g_J = 2J+1$, $g_{J+1} = 2(J+1)+1$

$$C' = K_{23} + K_{21} + \sigma_{2Jx} + 4\pi A_{2J1J+1}$$

$$E' = K_{21} - K_{01} + 4\pi A_{21}$$

$$F = K_{12} + K_{10} + K_{01} + 4\pi A_{10}$$

$$\gamma_1 = K_{32} + 2C' + \sigma_{2J}\,\mathrm{erf}(b) + F - BK_{12}\,\mathrm{erf}(b) + \sigma_{2Jx}(B\,\mathrm{erf}(b) - 1)$$

$$\gamma_2 = F\{K_{32} + 2C' + \sigma_{2J}\,\mathrm{erf}(b) + \sigma_{2Jx}(B\,\mathrm{erf}(b) - 1)\} + K_{32}\{2C' + (K_{23} + \sigma_{2Jx})(B\,\mathrm{erf}(b) - 1) + \sigma_{2J}\,\mathrm{erf}(b) - BK_{12}\,\mathrm{erf}(b)\} - K_{12}B\,\mathrm{erf}(b)(2C' + \sigma_{2J}) + K_{12}E'(\mathrm{erf}(b)B - 1) + \sigma_{2Jx}B\,\mathrm{erf}(b)(C' + \sigma_{2J}) + (C' - \sigma_{2Jx})(C' + \sigma_{2J}\,\mathrm{erf}(b))$$

$$\gamma_3 = F[K_{32}\{2C' + (K_{23} + \sigma_{2Jx})(B\,\mathrm{erf}(b) - 1) + \sigma_{2J}\,\mathrm{erf}(b)\} + C'\{C' + \sigma_{2Jx}(B\,\mathrm{erf}(b) - 1) + \sigma_{2J}\,\mathrm{erf}(b)\} + \sigma_{2J}\sigma_{2Jx}\,\mathrm{erf}(b)(B-1)] + C'[K_{32}\{C' + (K_{23} + \sigma_{2Jx})(B\,\mathrm{erf}(b) - 1) + \sigma_{2J}\,\mathrm{erf}(b) - 2BK_{12}\,\mathrm{erf}(b)\} - K_{12}B\,\mathrm{erf}(b)C' + \sigma_{2J} - E') - E'K_{12}] + K_{32}[\sigma_{2J}\,\mathrm{erf}(b)(B-1)(K_{23} + \sigma_{2Jx}) - E'K_{12} + K_{12}B\,\mathrm{erf}(b)(E' - \sigma_{2J})] + \sigma_{2J}E'K_{12}\,\mathrm{erf}(b)(B-1)$$

$$\gamma_4 = K_{32}[FC'\{C' + \sigma_{2J}\,\mathrm{erf}(b) + (K_{23} + \sigma_{2Jx})(B\,\mathrm{erf}(b) - 1)\} - K_{12}C'\{C'B\,\mathrm{erf}(b) + \sigma_{2J}B\,\mathrm{erf}(b) - E'(B\,\mathrm{erf}(b) - 1)\} + F\sigma_{2J}\,\mathrm{erf}(b)(B-1)(K_{23} + \sigma_{2Jx}) + K_{12}E'\sigma_{2J}\,\mathrm{erf}(b)(B-1)]$$

$$\alpha_{41} = -K_{32}B\,\mathrm{erf}(b)K_{01}N_\alpha K_{12}C'(C' + \sigma_{2J})$$

$$\alpha_{42} = \frac{G(0)2\pi b v_{2J1J+1}^2 \Delta v_D}{A_{2J1J+1}c^2(\ell n 2)^{1/2}}(C' + \sigma_{2J})C'K_{32}\{F(K_{21} + 4\pi A_{2J1J+1}) - E'K_{12}\} \equiv (G(0)/h\nu_{2J1J+1})\,\alpha'_{42}$$

$$N_\alpha = n_0 + n_1 + n_2$$

## Appendix II: Constants at pressure = 5.6 torr

$n_4^- = 2.0 \times 10^{16}$cm$^{-3}$, $n_3^- = 0.74 \times 10^{16}$cm$^{-3}$

$n_2^- = 1.22 \times 10^{16}$cm$^{-3}$, $n_1^- = 0.32 \times 10^{16}$cm$^3$

$n_0^- = 3.94 \times 10^{16}$cm$^{-3}$, $T_0 = 300$K, $T_1 = 350$K

$S_{21} = 2.44 \times 10^2$cm$^2$/J, $S_{12} = 2.28 \times 10^2$cm$^2$/J

$k_{21} = 9.44 \times 10^2$sec$^{-1}$, $k_{10} = 5.52 \times 10^3$sec$^{-1}$

$k_{32} = 2.12 \times 10^4$sec$^{-1}$, $k_{34} << k_{32}$ $(k_{23} \approx 0)$

$k_{12} = 7$ sec$^{-1}$ $k_{01} = 2.24 \times 10^2$sec$^{-1}$

$k_{23} = 1.18 \times 10^4$sec$^{-1}$ $\alpha = 1.359 \times 10^4$sec$^{-1}$

$B'' = 0.3874$ $t_{spont.} = 5.38$ sec

$a_1 = 0.04$

viscosity of mixture[18] $= 168.3 \times 10^{-6}$gm cm$^{-1}$sec$^{-1}$

$\sigma_{2J} = 4.44 \times 10^7$sec$^{-1}$

$\sigma_{2Jx} = 4.86 \times 10^7$ sec$^{-1}$ (Refs. 16, 17)

$(2RT_0)^{1/2} = 336$ m/sec

$c = 2.998 \times 10^{10}$ cm/sec

$h = 6.6262 \times 10^{-34}$ joules/sec

$B = (n_{2J}/n_2)_{eqm} = 0.0685$

## References


[1] Cool, T.A., "Power and Gain Characteristics of High Speed Flow Lasers," *Journal of Applied Physics,* Vol. 40, Aug. 1969, pp. 3563-3573.

[2] Bullis, R.H., Nighan, W.L., Fowler, M.C., and Weegand, W.J., "Physics of Electric Discharge Lasers," *AIAA Journal,* Vol. 10, Apr. 1972, pp. 407-414.

[3] Masson, H.A. and Bordeau, T.W., "Analyses of an Electric Discharge $CO_2$ Mixing Laser," *AIAA Journal,* Vol. 10, Apr. 1973, pp. 410-420.

[4] Anderson, J.D., Jr. and Harris, E.L., "Modern Advances in the Physics of Gas Dynamic Lasers," AIAA Paper 72-143, *AIAA Tenth Aerospace Sciences Meeting,* San Diego, Calif., 1972.

[5] Bennett, W.R., Jr., "Hole Burning Effects in a He-Ne Optical Maser," *Lasers: A Collection of Reprints with Commentary,* edited by J. Weber, Vol. 10A, Gordon & Breach, New York, 1968, pp. 688-701.

[6] Gordon, E.I., White, A.D., and Rigden, J.D., "Gain Saturation at 3.39 Microns in the He-Ne Maser," *Symposium on Optical Masers,* Polytechnic Institute of Brooklyn, April 1963, pp. 309-318.

[7] Rigrod, W. W., "Saturation Effects in High Gain Lasers," *Journal of Applied Physics*, vol. 36, Aug. 1965, pp. 2481-2490.

[8] Cool, T.A. and Shirley, J.A., "Gain Measurements in a Fluid Mixing $CO_2$ Laser System," *Applied Physics Letters,* Vol. 14, Jan. 1969, pp. 70-72.

[9] Cipolla, J.W. and Morse, T.F., "Kinetic Theory of an Optically Pumped Gas," *The Physics of Fluids,* Vol. 14, Sept. 1971, pp. 1850-1862.

[10] Healy, J.J. and Morse, T.F., "Theory of an Optically Pumped Gas Laser," *Journal of Quantititative Spectroscopy and Radiative Transfer,* Vol. 13, Sept. 1972, pp. 235-254.

[11] Healy, J.J. and Morse, T.F., "Cavity Detuning and Multimode Operation of an Optically Pumpted Gas Laser," *Physical Review,* Vol. 6, Dec. 1972, pp. 2457-2469.

[12] Cabezas, A.Y. and Treat, R.P., "Effect of Spectral Hole-Burning and Cross Relaxation on the Gain Saturation of Laser Amplifiers," *Journal of Applied Physics,* Vol. 37, Aug. 1966, pp. 3556-3563.

[13] Gerry, E.T. and Leonard, D.A., "Measurements of 10.6 $\mu$ $CO_2$ Laser Transition Probability and Optical Broadening Cross Sections," *Applied Physics Letters,* Vol. 8, May 1, 1966, pp. 227-229.

[14] Murray, E.R., Kruger,C., and Mitchner, M., "Measurement of 9.6 $\mu$ $CO_2$ Laser Transition Probability and Optical Broadening Cross Section," *Applied Physics Letters*, Vol. 24, No. 4, Feb. 15, 1974, pp. 180-181.

[15] Abrams, R.L., "Broadening Coefficients for the P(20) $CO_2$ Laser Transition," *Applied Physics Letters,* Vol. 25, No. 10, Nov. 15, 1974, pp. 609-611.

[16] Jacobs, R.R., Pettipiece, K.J., and Thomas, S.J., "Rotational Relaxation Rate Constants for $CO_2$," *Applied Physics Letters,* Vol. 24, No. 8, April 15, 1974, pp. 375-377.

[17] Cheo, P.K., "$CO_2$ Lasers," *Lasers—Series of Advances,* Vol. III, Marcel Dekker, Inc., New York, 1971, pp. 111-267.

[18] Kestin, J. and Mason, E.A., "Transport Properties in Gases," *Transport Phenomena—1973*, edited by J. Kestin, AIP Conference Proceedings #11, American Institute of Physics, New York, 1973, pp. 137-192.

[19] Kan, T. and Wolga, G.J., "Influence of Collisions on Radiative Saturation and Lamb Dip Formation in $CO_2$ Molecular Lasers," *IEEE Journal of Quantum Electronics*, Vol. QE-7, April 1971, pp. 141-150.